

# Entangling macroscopic light states by delocalized photon addition

Nicola Biagi<sup>1,2</sup>, Luca S. Costanzo<sup>1,2</sup>, Marco Bellini<sup>1,2\*</sup>, and Alessandro Zavatta<sup>1,2\*</sup>

<sup>1</sup>*Istituto Nazionale di Ottica (CNR-INO), L.go E. Fermi 6, 50125 Florence, Italy*

<sup>2</sup>*LENS and Department of Physics & Astronomy,  
University of Firenze, 50019 Sesto Fiorentino, Florence, Italy*

(Dated: November 27, 2018)

We present the experimental generation of tunable entanglement between distinct field modes by the delocalized addition of a single photon. We show that one can preserve a high degree of entanglement even between macroscopically populated modes and illustrate this concept by adding a single photon to two modes containing identical coherent states of growing amplitude. Discorrelation, a new joint statistical property of multimode quantum states, is also experimentally demonstrated here for the first time.

Keywords:

Entanglement is a distinctive feature of quantum mechanics marking the most striking deviations of its predictions from those of classical physics. Entanglement has now been widely experimentally demonstrated in several microscopic systems, with recent achievements including the loophole-free violation of Bell's inequalities [1, 2]. However, entangling larger and larger objects is an increasingly difficult task [3]. Its realization would allow one to test fundamental decoherence and wavefunction collapse theories [4, 5] that try to explain why we do not normally observe quantum superpositions and entanglement in our everyday life.

Recent optical experiments have approached this question by generating so-called 'micro-macro' entanglement [6, 7] where one part of a system in a microscopic superposition of vacuum and one-photon states is entangled with another part containing a macroscopic mean number of photons.

Here we propose and test a different scheme that allows us to produce tunable entanglement between two states, both containing arbitrarily large numbers of photons. Our basic ingredient is the possibility of performing the coherent delocalized addition of a single photon over different modes. This 'macro-macro' kind of entanglement is shown to be independent of the size of the entangled partners and particularly robust against losses.

Photon addition (by the creation operator  $\hat{a}^\dagger$ ) and subtraction (by the annihilation operator  $\hat{a}$ ) have already demonstrated to be extremely useful for performing operations normally unavailable in the realm of Gaussian quantum optics [8–10]. Photon subtraction from a single-mode photonic state can de-Gaussify it [11] and enhance its non-classicality [12]. Moreover, it can increase and distill existing two-mode entanglement [13, 14]. On the other hand, photon addition has the unique capability of creating (single-mode) non-classicality [15, 16] and (multi-mode) entanglement, whatever the input states.

In particular, the coherent addition of a single photon to two distinct field modes, 1 and 2, entangles them, and the entanglement produced by a balanced superposition of the kind  $\hat{a}_1^\dagger + e^{i\varphi}\hat{a}_2^\dagger$  depends on the states of light al-

ready present in the two modes before the operation. If both are originally in a vacuum state, one simply obtains a single-photon mode-entangled state [17] of the kind  $|\psi\rangle_{12} = (|1\rangle_1|0\rangle_2 + e^{i\varphi}|0\rangle_1|1\rangle_2)/\sqrt{2}$ . If different quantum states originally populate the field modes, the state resulting from delocalized photon addition may present different features. For example, injecting a vacuum and a coherent state in the two input modes give rise to a so-called hybrid discrete/continuous-variable entanglement of the two output modes [18].

Here we study the effect of delocalized single-photon addition on two input modes containing identical coherent states  $|\alpha\rangle$ , as schematically illustrated in Fig.1. The

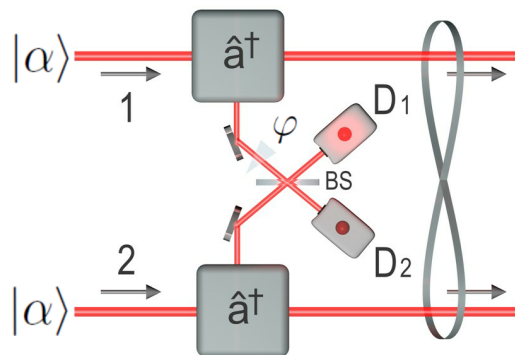


FIG. 1: Simplified experimental scheme to perform a coherent single-photon addition on two different input modes, both containing a coherent state  $|\alpha\rangle$ . A click in a single-photon detector  $D_1$ , placed after a balanced beam-splitter BS mixing the herald modes of two photon-addition modules based on parametric down-conversion (PDC) [10, 15], generates entanglement between the two output modes.

general entangled state produced by this operation can be written as:

$$\begin{aligned} |\psi_\varphi(\alpha)\rangle_{12} &= \left( \hat{a}_1^\dagger |\alpha\rangle_1 |\alpha\rangle_2 + e^{i\varphi} |\alpha\rangle_1 \hat{a}_2^\dagger |\alpha\rangle_2 \right) / \sqrt{\mathcal{N}} \\ &= \left[ \hat{D}_1(\alpha) \hat{D}_2(\alpha) \left( |1\rangle_1 |0\rangle_2 + e^{i\varphi} |0\rangle_1 |1\rangle_2 \right) \right. \\ &\quad \left. + \alpha^* (1 + e^{i\varphi}) |\alpha\rangle_1 |\alpha\rangle_2 \right] / \sqrt{\mathcal{N}} \end{aligned} \quad (1)$$

with the normalization factor  $\mathcal{N} = 2[1 + |\alpha|^2(1 + \cos \varphi)]$  and the phase-space displacement operator  $\hat{D}(\alpha) = e^{\alpha \hat{a}^\dagger - \alpha^* \hat{a}}$ . Already in this simple case of balanced photon addition, the output state shows a very rich structure resulting from the coherent contribution of an entangled and a separable part with adjustable weights depending on the superposition phase  $\varphi$  and on the amplitude  $\alpha$  of the coherent states.

It is easy to see that, in the extreme case of an even superposition with  $\varphi = 0$ , the degree of entanglement of the state (quantified via the negativity of the partial transpose, NPT [19]) quickly deteriorates for increasing  $\alpha$ , due to the large contribution of the separable fraction in Eq.(1). However, the entangled contribution can

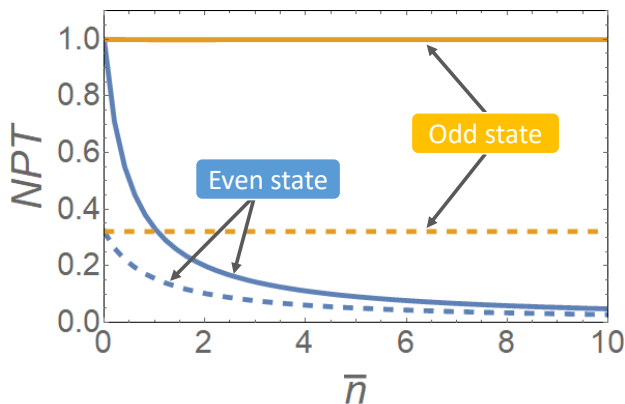


FIG. 2: Theoretical entanglement (quantified via the negativity of the partial transpose, NPT) of the odd and even entangled states (yellow and blue curves, respectively). Dashed curves present the NPT behavior when both the modes are subjected to 40% of losses.

be continuously increased by varying the superposition phase  $\varphi$ , until the other extreme condition of  $\varphi = \pi$  is reached. In this case, the odd superposition entangled state

$$|\psi_\pi(\alpha)\rangle_{12} = \frac{1}{\sqrt{2}}(\hat{a}_1^\dagger |\alpha\rangle_1 |\alpha\rangle_2 - |\alpha\rangle_1 \hat{a}_2^\dagger |\alpha\rangle_2), \quad (2)$$

is seen to be equivalent to the result of an equal phase-space displacement operation  $\hat{D}(\alpha)$  on both modes of a single-photon mode-entangled state. As such, it is expected to maintain constant entanglement independently of the amplitude of the input coherent states (see Fig.2). Ideally, a high degree of entanglement should thus be observable in the  $|\psi_\pi(\alpha)\rangle$  state even between two modes containing large, and possibly macroscopic, mean photon numbers  $\bar{n} = |\alpha|^2$ . More interestingly, this behavior is preserved even when the states are affected by channel transmission losses and detection inefficiency, as shown by the dashed curves of Fig. 2.

The odd superposition entangled states (2) are therefore an exceptional test-bed for studying the robustness

and detectability of entanglement for states of growing macroscopicity, and their properties have already been theoretically discussed in Ref.[20]. The 'micro-macro' entanglement experiments of [6, 7] are scaled-down realizations of such a proposal, where displacement is performed on just one of the two modes. Moreover, entanglement is finally verified by 'un-doing' the macroscopicity and optically displacing the state back to the ( $|0\rangle$ ,  $|1\rangle$ ) Fock subspace before measurements, as recently done in Ref.[21].

Differently from the approaches of Refs.[6, 7], here we generate real tunable 'macro-macro' entanglement. Furthermore, we perform a complete two-mode homodyne detection of the states, in principle allowing us to directly evaluate their entanglement for arbitrary macroscopicity.

We use the temporal-mode version (see Fig.3) of the setup illustrated in Fig.1 for generating states of the form of Eq.(2) experimentally. In this case, the two devices for single-photon addition are replaced by a single one, operating on two different traveling temporal modes. The coherent superposition of photon additions on mode 1 or 2 is obtained by allowing the herald photon from the addition device (based on stimulated PDC [10]) to travel two indistinguishable paths of different length towards the herald detector [17].

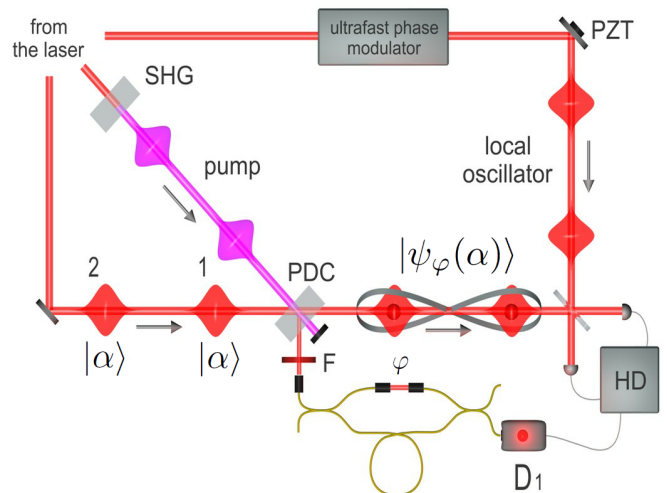


FIG. 3: Schematic view of the temporal-mode version of the experimental setup performing coherent single-photon addition on two different input temporal modes, both containing a coherent state  $|\alpha\rangle$ . A click in the single-photon detector  $D_1$ , placed after a Mach-Zehnder interferometer unbalanced by the time delay between the input temporal modes, heralds the production of the entangled state of Eq.(2) in the two output modes. Symbols are defined in the text.

In principle, besides its higher phase stability, the temporal-mode version of the experiment has the fundamental additional advantage of an easy scalability, because it allows one to increase the number of involved

modes without a corresponding multiplication of photon addition devices and detectors.

We inject several coherent state amplitudes  $\alpha$  at the input, and perform a quantum tomographic analysis of the final output states based on time-multiplexed homodyne detection, where an ultrafast modulator controls the phases of the two local oscillator (LO) pulses in the separate temporal modes (more details in the Methods section). The reconstructed two-mode density matrices are then used to calculate their NPT and extract the degree of entanglement of the states as a function of their macroscopicity.

At this point, it is worth noting that a faithful representation of states like those of Eq. (2) requires the reconstruction of a number of density matrix elements that grows extremely fast with the coherent state amplitude  $|\alpha|$ . For example, already for  $|\alpha| \approx 7$ , corresponding to a mean photon number of  $\bar{n} = |\alpha|^2 \approx 50$  photons per mode, at least  $3 \times 10^7$  density matrix elements need to be calculated. Since the brute force approach of full density matrix reconstruction has no hope to succeed with such a huge number of elements, we adopt two different strategies to restrict the reconstructed subspace.

In the first method, the global LO phase for homodyne detection is actively randomized while the relative phase between the two temporal LO modes is scanned in a controlled way over 9 different values. About 50,000 quadrature measurements per mode are performed for each value of the relative LO phase, and only the density matrix elements diagonal with respect to the LO global phase are then reconstructed by means of an iterative maximum likelihood algorithm [23, 24]. Figure 4a shows that measured NPT values for such a phase-averaged tomography agree very well with theoretical expectations. It is interesting to note that, while global phase averaging lowers the NPT of the state, entanglement is still well preserved also for large mean photon numbers. Although the number of density matrix elements to reconstruct is considerably reduced with respect to the full tomography case, the largest state that we can analyze with this method has a mean photon number per mode  $\bar{n} \approx 6$ , mainly due to finite computational resources (an optimized parallel code running on a 8-CPU 3.4-GHz Xeon processor requires more than 70 hours to reconstruct a  $\bar{n} = 6$  odd state).

These limitations can be overcome by using a different approach, where the global LO phase is kept fixed and we numerically filter out the mean field component from quadrature measurements. This “ac-tomography” relies on the fact that the entanglement features of the odd state (2) derive from those of a displaced delocalized single photon and are therefore entirely contained in the correlated fluctuations of the quadrature measurements of the two modes around their common mean values. Again, about 50,000 quadrature values are acquired for 9 different relative LO phases when the global LO

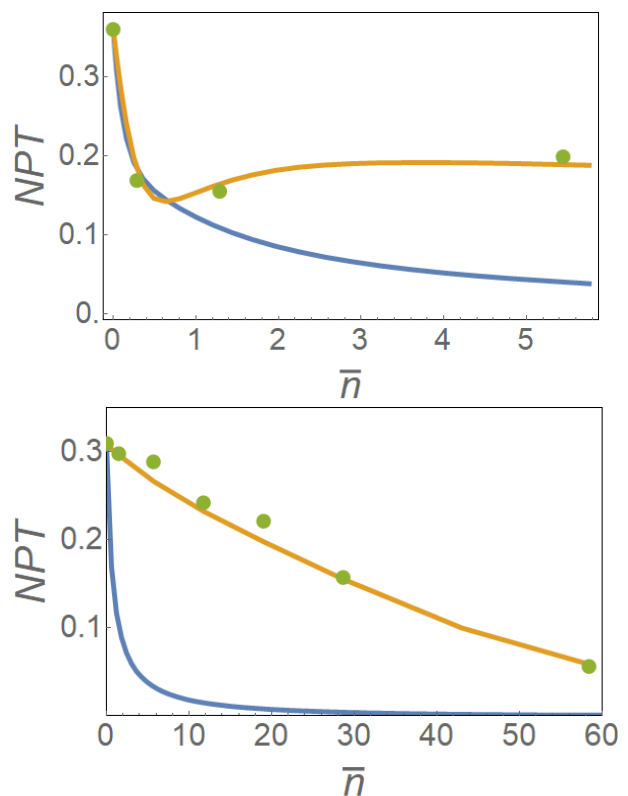


FIG. 4: Experimental (green dots) and calculated NPT for the odd entangled states (yellow solid curves) as a function of the mean photon number  $\bar{n}$  (the calculated NPT curves for even entangled states are also shown in blue for reference). Upper panel: “global-phase-averaged tomography”. The theoretical curves are calculated with a detection efficiency  $\eta = 68\%$ . Bottom panel: “ac-tomography” shows significant entanglement between modes with up to about 60 photons each. The theoretical curve is calculated by considering a detection efficiency  $\eta = 64\%$  together with a noise of  $\pi/100$  on both the state phase  $\varphi$  and the LO global phase. In addition, the observed value of entanglement is mainly limited by the state preparation efficiency, degrading with increasing mean photon number due to a non-perfect Mach-Zehnder visibility of 99.6%.

phase is now locked to zero. By subtracting the means of the measured quadrature distributions, we thus numerically displace the state back towards the phase-space origin before tomographically reconstructing the two-mode density matrix in the subspace of zero, one and two photons. This approach has two main advantages. On one hand, the macroscopic state is fully detected by the homodyne detector and no extra optical displacements are required, thus avoiding unwanted phase and amplitude noise in the final state [20]. On the other hand, the reconstructed space is maintained fixed regardless of the state macroscopicity, thus allowing the analysis of very large states.

Results are shown in Fig. 4b. Compared to the ideal

constant behavior of the theoretical NPT for the odd state shown in Fig.2, the experimental NPT shows an unexpected decrease for growing  $\bar{n}$ , but the analyzed states nonetheless preserve a relatively large degree of entanglement even for macroscopic mean photon numbers (up to  $\bar{n} \approx 60$ ) in each mode. The observed degradation of the experimental NPT can be fully accounted for by including the effects of phase instabilities and limited detection and preparation efficiency. The latter has the most important effect, mixing of the desired odd entangled state with a separable pair of coherent states of the same amplitude.

Besides its interesting entanglement properties, the odd entangled state (2) generated by delocalized single-photon addition onto a pair of coherent states presents another peculiarity in its joint photon number probability distribution. As shown by the null diagonal in the theoretical plot of Fig. 5b, the number of photons in each of the two modes can take any value individually, but the two modes together never exhibit the same. This should be compared to the case of the original two-mode coherent states, also shown in Fig. 5a, where the maximum joint probability lies on the diagonal instead. This so-called *discorrelation* property was first discussed in [25] and, opposite to quantum key distribution schemes where common random keys need to be shared, it can be used to distribute unique randomness between parties. The joint photon number distribution obtained from an experimental density matrix in the case  $\alpha \simeq 2$  is shown Fig. 5c. Although it does not exhibit the perfect discorrelation of the ideal state due to experimental imperfections, it nevertheless presents a clear decrease of the diagonal elements. This is better illustrated in Fig. 5d, where the integral of the three joint photon number distributions of Figs. 5a-c along the diagonal direction are presented. It therefore shows the probability of a difference  $\Delta n = n_1 - n_2$  in the photon counts between the two modes. While the ideal separable  $|\alpha\rangle_1|\alpha\rangle_2$  state shows a maximum, the measured odd entangled state corresponding to Eq.(2) has a pronounced local minimum for  $\Delta n = 0$ , a clear signature of discorrelation.

In conclusion, we have demonstrated a new versatile method, based on the delocalized addition of a single photon, to generate arbitrarily tunable entanglement between states of arbitrarily large size. The remarkable simplicity of our scheme will probably make it an invaluable tool for investigating the transition of quantum phenomena between the microscopic and macroscopic regimes. By analyzing the particular case of an odd superposition of photon addition operations onto identical coherent states, we have experimentally verified entanglement between modes populated with a mean photon number up to about 60. This kind of 'macro-macro' entanglement has been shown to be particularly robust against losses and is thus well suited for quantum communication tasks and storage in atomic quantum memories. Furthermore,

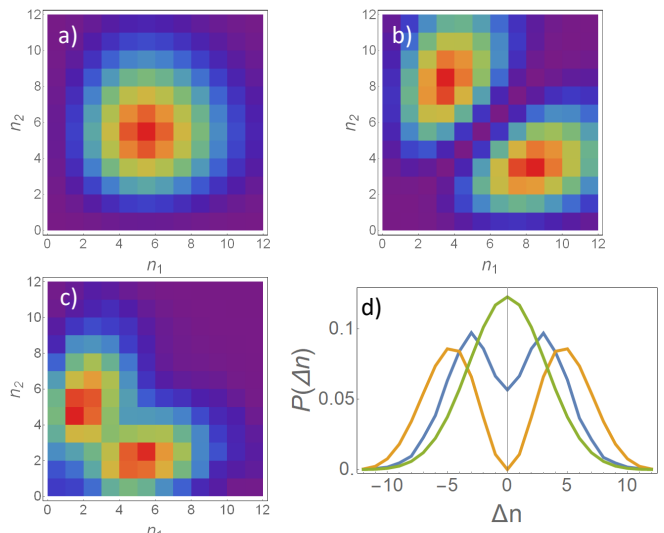


FIG. 5: Joint photon number distributions for: a) an ideal separable  $|\alpha\rangle_1|\alpha\rangle_2$  state; b) the ideal odd entangled state of Eq.(2); c) the experimental odd entangled state as reconstructed by global-phase-averaged tomography. For all the plots,  $\alpha \simeq 2$  has been used. d) probability of a difference  $\Delta n = n_1 - n_2$  in the photon counts between the two modes for the three above cases: a) green ; b) yellow; c) blue.

the peculiar statistical property of discorrelation, experimentally verified here for the first time, might make these states useful for specific applications, such as distributed voting schemes [26] or fair card dealing in “mental poker” games [27, 28].

## METHODS

The experimental setup, schematically shown in Fig. 3, is based on a mode-locked laser emitting 1.5-ps pulses at 786 nm and with a repetition rate of 81 MHz, which provides the following beams: the local oscillator (LO) for homodyne detection, the pump for a parametric down-conversion (PDC) process after a frequency-doubling stage (SHG), and the seed coherent states for photon addition in the PDC crystal. PDC photons emitted in the idler channel pass through a set of spectral and spatial filters (F) before entering an unbalanced, fiber-based, Mach-Zehnder interferometer. A detection event by the single-photon detector ( $D_1$ ) placed at one of the interferometer outputs announces the successful implementation of a delocalized single-photon addition, meaning that entanglement has been conditionally generated between the two temporal modes. The state superposition phase  $\varphi$  is remotely controlled by varying the relative phase between the interferometer arms via a fine adjustment of an air-gap length. A feedback loop based on the interference of a counter-propagating pulse train injected in the unused interferometer output port provides phase

stabilization.

In order to perform state characterization by quantum tomography, two-mode time-domain homodyne detection is performed. The phases of the two local oscillator pulses are independently changed in the  $[0, \pi]$  interval by controlling their global phase via a piezo-mounted mirror (PZT), and their relative phase by means of an ultrafast electro-optic modulator driven with a sine wave at 20.2 MHz. Actually, the Mach-Zehnder interferometer is unbalanced by twice the inverse of the laser repetition rate in order to prepare the entangled state over two non-consecutive pulses and therefore avoid any possible cross-talk between the temporal modes due to the limited bandwidth of the homodyne detector [22].

### ACKNOWLEDGMENTS

The authors gratefully acknowledge the support of Ente Cassa di Risparmio di Firenze and of the Italian Ministry of Education, University and Research (MIUR), under the 'Progetto Premiale: QSecGroundSpace'.

- 
- [1] M. Giustina et al., Significant-Loophole-Free Test of Bells Theorem with Entangled Photons, *Phys. Rev. Lett.* **115**, 250401 (2015).
- [2] L.K. Shalm et al., Strong Loophole-Free Test of Local Realism, *Phys. Rev. Lett.* **115**, 250402 (2015).
- [3] F. Fröwis, P. Sekatski, W. Dür, N. Gisin, and N. Sangouard, Macroscopic quantum states: Measures, fragility, and implementations, *Rev. Mod. Phys.* **90**, 025004 (2018).
- [4] W.H. Zurek, Decoherence, einselection, and the quantum origins of the classical, *Rev. Mod. Phys.* **75**, 715 (2003).
- [5] M. Arndt and K. Hornberger, Testing the limits of quantum mechanical superpositions, *Nat. Phys.* **110**, 271 (2014).
- [6] N. Bruno, A. Martin, P. Sekatski, N. Sangouard, R. T. Thew, and N. Gisin, Displacement of entanglement back and forth between the micro and macro domains, *Nat. Phys.* **9**, 545 (2013).
- [7] A. I. Lvovsky, R. Ghobadi, A. Chandra, A. S. Prasad, and C. Simon, Observation of micromacro entanglement of light, *Nat. Phys.* **9**, 541 (2013).
- [8] L. S. Costanzo, A. S. Coelho, N. Biagi, J. Fiurek, M. Bellini, and A. Zavatta, Measurement-Induced Strong Kerr Nonlinearity for Weak Quantum States of Light, *Phys. Rev. Lett.* **119**, 013601 (2017).
- [9] A. Zavatta, J. Fiurasek, and M. Bellini, A high-fidelity noiseless amplifier for quantum light states, *Nat. Phot.* **5**, 52 (2011).
- [10] M. Bellini, and A. Zavatta, Manipulating light states by single-photon addition and subtraction, *Prog. Opt.* **55**, 41 (2010).
- [11] J. Wenger, R. Tualle-Brouri, and P. Grangier, Non-Gaussian Statistics from Individual Pulses of Squeezed Light, *Phys. Rev. Lett.* **92**, 153601 (2004).
- [12] A. Ourjoumtsev, R. Tualle-Brouri, J. Laurat, and P. Grangier, Generating Optical Schrödinger Kittens for Quantum Information Processing, *Science* **312**, 83 (2006).
- [13] A. Ourjoumtsev, A. Dantan, R. Tualle-Brouri, and P. Grangier, Increasing entanglement between Gaussian states by coherent photon subtraction, *Phys. Rev. Lett.* **98**, 030502 (2007).
- [14] H. Takahashi, J. Neergaard-Nielsen, M. Takeuchi, M. Takeoka, K. Hayasaka, A. Furusawa, M. and Sasaki, Entanglement distillation from Gaussian input states, *Nat. Phot.* **4**, 178 (2010).
- [15] A. Zavatta, S. Viciani, and M. Bellini, Quantum-to-classical transition with single photon-added coherent states of light, *Science* **306**, 660 (2004).
- [16] S. Rahimi-Keshari, T. Kiesel, W. Vogel, S. Grandi, A. Zavatta, and M. Bellini, Quantum Process Nonclassicality, *Phys. Rev. Lett.* **110**, 160401 (2013).
- [17] A. Zavatta, M. D'Angelo, V. Parigi, and M. Bellini, Remote preparation of arbitrary time-encoded single-photon ebits, *Phys. Rev. Lett.* **96**, 020502 (2006).
- [18] H. Jeong, A. Zavatta, M. Kang, S. Lee, L.S. Costanzo, S. Grandi, T.C. Ralph, and M. Bellini, Generation of hybrid entanglement of light, *Nat. Photon.* **8**, 564 (2014).
- [19] J. Lee, M. S. Kim, Y. J. Park, and S. Lee, *J. Mod. Opt.* **47**, 2151 (2000).
- [20] P. Sekatski, N. Sangouard, M. Stobińska, F. Bussières, M. Afzelius, and N. Gisin, Proposal for exploring macroscopic entanglement with a single photon and coherent states, *Phys. Rev. A* **86**, 060301(R) (2012).
- [21] D.V. Sychev, V. A. Novikov, K.K Pirov, E.S. Tiunov, C. Simon, and A.I. Lvovsky, Entanglement of macroscopically distinct states of light, arXiv:1811.01041v2 (2018).
- [22] A. Zavatta, M. Bellini, P.L. Ramazza, F. Marin, and F.T. Arecchi, *J. Opt. Soc. Am. B* **19**, 1189 (2002).
- [23] Z. Hradil, J. Řeháček, J. Fiurášek, and M. Ježek, in Quantum State Estimation, edited by M. Paris and J. Řeháček, Lecture Notes in Physics Vol. **649** (Springer, Berlin, 2004).
- [24] A.I. Lvovsky, Iterative maximum-likelihood reconstruction in quantum homodyne tomography, *J. Opt. B Quantum Semiclassical Opt.* **6**, S556 (2004).
- [25] E. Meyer-Scott, J. Tiedau, G. Harder, L. K. Shalm, and T. J. Bartley, Discorrelated quantum states, *Sci. Rep.* **7**, 41622 (2017).
- [26] J.-M. Bohli, J. Mller-Quade and S. Rhrich, Bingo voting: Secure and coercion-free voting using a trusted random number generator. In A. Alkassar and M. Volkamer (eds) E-Voting and Identity, 111124 (Springer Berlin Heidelberg, 2007).
- [27] P. Golle, Dealing cards in poker games. In Proceedings of the International Conference on Information Technology: Coding and Computing vol. 1, 506511 (2005).
- [28] A. Shamir, R. L. Rivest and L. M. Adleman, Mental poker. In D. A. Klarner (ed.) The Mathematical Gardner, 3743 (Springer, Boston, 1981)